JOURNAL

OF THE AMERICAN CHEMICAL SOCIETY

VOLUME 104, NUMBER 23 NOVEMBER 17, 1982

Quantum Chemical Studies of a Model for Peptide Bond Formation: Formation of Formamide and Water from Ammonia and Formic Acid

Tetsuro Oie,[†] Gilda H. Loew,*[†] Stanley K. Burt,[‡] J. Stephen Binkley,[§] and Robert D. MacElroy[∥]

Contribution from The Rockefeller University, Molecular Theory Laboratory, Palo Alto, California 94304, Molecular Research Institute, Palo Alto, California 94304, Sandia National Laboratories, Division 8341, Livermore, California, and NASA Ames Research Center, Moffett Field, California 94035. *Received December 10, 1981*

Abstract: The S_N2 reaction between ammonia and formic acid has been studied as a model reaction for peptide bond formation using the semiempirical MNDO and ab initio molecular orbital methods. Two reaction mechanisms have been examined, i.e., a stepwise and a concerted reaction. The stationary points of each reaction including intermediate and transition states have been identified and free energies have been calculated for all geometry optimized reaction species to determine the thermodynamics and kinetics of each reaction. The stepwise mechanism was found to be more favorable than the concerted one by both MNDO and ab initio calculations. However, the ab initio method predicts both mechanisms to be fairly competitive with free energies of activation of about 50 kcal/mol. Despite excellent agreement between both methods in the calculated entropies and thermal energies, the minimum basis set character of MNDO leads to values of free energy of activation much higher than those obtained by the ab initio method. The basis set dependence and effect of correlation of the computed ab initio results and the relative effects of polarization and correlation were also investigated by using a number of basis sets up to 6-31G** and estimates of correlation energy by Møller–Plesset perturbation theory up to fourth order. Correlation energy was found to be a significant factor in the stabilization of transition states.

Introduction

The origin of life most probably occurred as part of a sequence of chemical processes driven by energy in the environment of the primitive earth and constrained by the physical conditions of that environment. For life to develop, there are a number of important processes that must have occurred, such as synthesis of relevant monomeric compounds (e.g., amino acids and nucleotides), polymerization of these monomers, and the replication of polymers to form reasonably accurate copies of the original molecules.

One of the major objectives in origin of life studies is to identify the significant events in the evolution of protein synthesis, from nondirected amino acid sequences, dependent on intrinsic factors such as monomer concentration, energy availability, and the intrinsic stereochemistry of the forming polymers, to extrinsically directed (templated) amino acid sequences. In approaching this objective, there have been numerous attempts[1] to synthesize polypeptides from their component amino acids under conditions that resemble those of the primitive earth. Attempts have been made to activate amino acids by a variety of methods including esterification, phosphorylation, and the presence of divalent cations (e.g., Mg^{2+}, Ca^{2+}, Zn^{2+}, Cu^{2+}, and Ni^{2+}). However, the design of effective experiments and the interpretation of results have been hampered by a lack of detailed information of the mechanism of peptide bond formation. Therefore we have begun a systematic study of this mechanism under a variety of conditions using the techniques of theoretical chemistry.

As a first step in understanding the mechanism of peptide bond formation, we report here the characterization of the amide bond formation between a neutral formic acid and ammonia. This

$$NH_3 + HCOOH \rightarrow NH_2CHO + H_2O$$

reaction should closely correspond to peptide bond formation between neutral amino acids or their alkyl esters. This reaction also represents some aspects of activation by esterification, since none of the amino acid forms (i.e., cationic, zwitterionic, and anionic) present in solution at any pH is a viable candidate for

[†] The Rockefeller University.
[‡] Molecular Research Institute.
[§] Sandia National Laboratories.
[∥] Nasa Ames Research Center.

(1) (a) Weber, A. L.; Orgel, L. E. *J. Mol. Evol.* **1981**, *17*, 190. (b) Lahav, N.; White, D. H. *Ibid.* **1980**, *16*, 11. (c) Weber, A. L.; Orgel, L. E. *Ibid.* **1980**, *16*, 1. (d) Mullins, D. W.; Lacey, J. C. *Ibid.* **1980**, *15*, 339. (e) Weber, A. L.; Orgel, L. E. *Ibid.* **1979**, *13*, 185. (f) Weber, A. L.; Orgel, L. E. *Ibid.* **1978**, *11*, 189. (g) Weber, A. L.; Orgel, L. E. *Ibid.* **1978**, *11*, 9. (h) Steinman, G.; Cole, M. N. *Proc. Natl. Acad. Sci. U.S.A.* **1967**, *58*, 735. (i) Steinman, G. *Arch. Biochem. Biophys.* **1967**, *121*, 533. (j) Steinman, G.; Kenyon, D. H.; Calvin, M. *Biochim. Biophys. Acta* **1966**, *124*, 339. (k) Ponnamperuma, C.; Peterson, E. *Science* **1965**, *147*, 1572. (l) Steinman, G.; Kenyon, D. H.; Calvin, M. *Nature (London)* **1965**, *206*, 707. (m) Steinman, G.; Lemmon, R. M.; Calvin, M. *Proc. Natl. Acad. Sci. U.S.A.* **1964**, *52*, 27. (n) Yamada, S.; Wagatsuma, M.; Takeuchi, Y.; Terashima, S. *Chem. Pharm. Bull.* **1971**, *19*, 2380. (o) Yamada, S.; Terashima, S.; Wagatsuma, M. *Tetrahedron Lett.* **1970**, 1501.

0002-7863/82/1504-6169$01.25/0

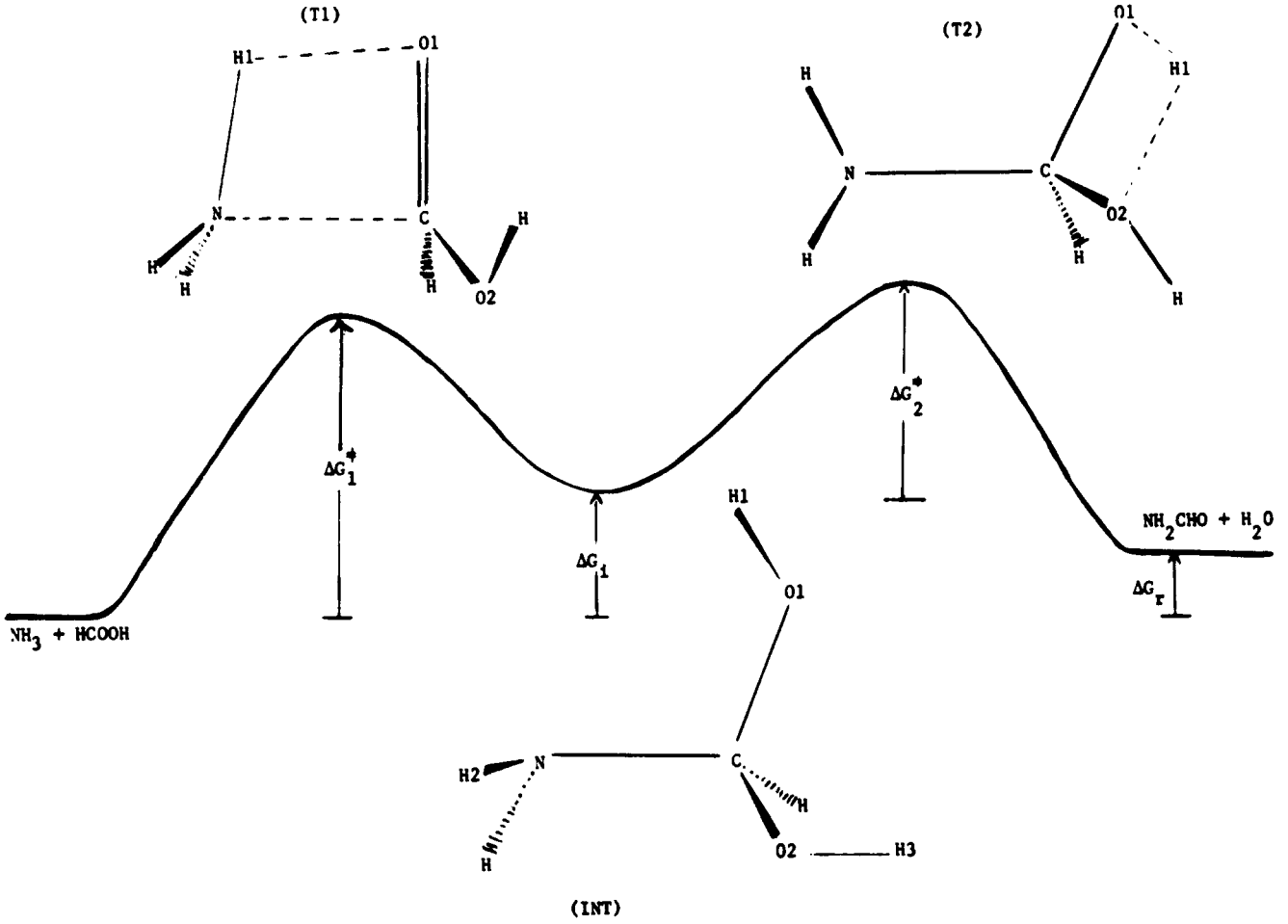

Figure 1. Stepwise reaction mechanism and free energy diagram of the reaction. See Table I for the optimized geometrical parameters of the transition states (T1), (T2), and intermediate (INT).

peptide bond formation because of the presence of the protonated amino or anionic carboxylate group, and only by ester formation does a neutral form of amino acids dominate in solution at neutral pH.[2]

Since there have been no theoretical studies reported for bimolecular substitution reactions of the complexity corresponding to peptide bond formation, or even of the model ammonia–formic acid reaction, we have initiated a fairly thorough investigation for this model reaction using both the semiempirical MNDO[3] and ab initio[4] methods. With the latter, a number of basis sets (STO-3G,[5] 3-21G,[6] 6-31G,[7] 6-31G*,[8] 6-31G**[8]) were used, as well as a Møller–Plesset perturbation approximation to electron correlation correction due to Pople.[9]

Theoretical studies by quantum mechanical methods can provide valuable information about the nature of the transition states and metastable intermediates, which cannot be readily characterized by experimental techniques. Such information, as well as details of the thermodynamics and kinetics of the reaction, thereby allows direct insight into reaction mechanisms providing that the data are complementary to, and consistent with, available experimental results.

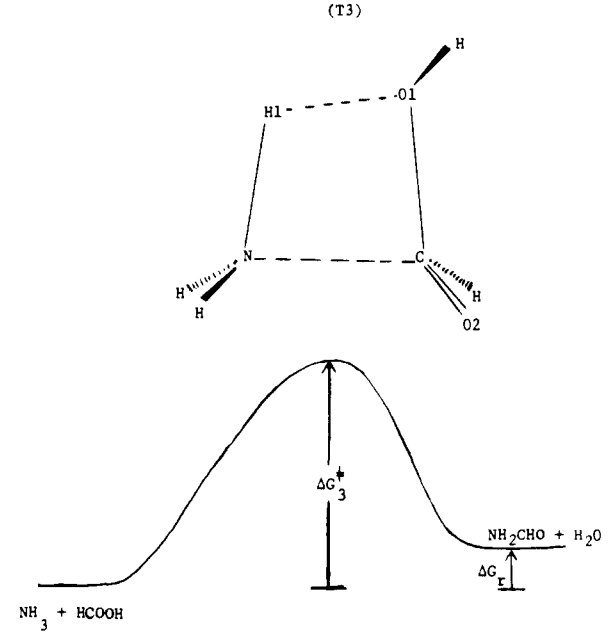

Figure 2. Concerted reaction mechanism and free energy diagram of the reaction. See Table I for the optimized geometrical parameters of the transition state (T3).

For the model amide bond formation, we have considered two possible mechanisms: a stepwise reaction (Figure 1) and a concerted reaction (Figure 2). In the first case, the reaction takes

(2) Hay, R. W.; Porter, L. J. *J. Chem. Soc.* **1967**, 1261.
(3) (a) Dewar, M. J. S.; Thiel, W. *J. Am. Chem. Soc.* **1977**, *99*, 4899. (b) Dewar, M. J. S.; Thiel, W. *Ibid.* **1977**, *99*, 4907.
(4) Binkley, J. S.; Whiteside, R. A.; Krishnan, R.; Seeger, R.; DeFrees, D. J.; Schlegel, H. B.; Topiol, S.; Kahn, L. R.; Pople, J. A. "Gaussian 80", QCPE 406, Indiana University.
(5) Hehre, W. J.; Stewart, R. F.; Pople, J. A. *J. Chem. Phys.* **1969**, *51*, 2657.
(6) Binkley, J. S.; Pople, J. A.; Hehre, W. J. *J. Am. Chem. Soc.* **1980**, *102*, 939.
(7) Hehre, W. J.; Ditchfield, R.; Pople, J. A. *J. Chem. Phys.* **1972**, *56*, 2257.
(8) Hariharan, P. C.; Pople, J. A. *Theor. Chim. Acta* **1973**, *28*, 213.
(9) (a) Møller, C.; Plesset, M. *Phys. Rev.* **1934**, *46*, 618. (b) Binkley, J. S.; Pople, J. A. *Int. J. Quantum Chem.* **1975**, *9*, 229. (c) Pople, J. A.; Binkley, J. S.; Seeger, R. *Int. J. Quantum Chem. Symp.* **1976**, *10*, 1. (d) Pople, J. A.; Krishnan, R.; Schlegel, H. B.; Binkley, J. S. *Int. J. Quantum Chem.* **1978**, *14*, 545.

Table I. Ab Initio and MNDO Optimized Structures of Transition States and Intermediate

molecule[a]	parameter[b]	MNDO	STO-3G	3-21G
(T1)	C–N	1.585	1.756	1.606
	C=O1	1.332	1.315	1.356
	C–O2	1.385	1.402	1.400
	H1–O1	1.406	1.404	1.362
	H1–N	1.237	1.128	1.216
	∠NCO1	91.0	89.9	93.9
	∠H1O1C	84.4	79.8	78.0
	∠H1NC	80.4	70.7	73.2
	∠NCO2	110.3	107.9	107.4
	τH1O1CN	−0.9	−0.4	2.8
(T2)	C–N	1.450	1.441	1.336
	C–O1	1.328	1.312	1.337
	C–O2	1.541	1.720	1.839
	H1–O1	1.399	1.377	1.189
	H1–O2	1.172	1.078	1.260
	∠NCO1	116.7	120.6	119.1
	∠O1CO2	89.2	88.1	84.5
	∠H1O1C	84.1	80.0	86.2
	∠H1O2C	83.4	72.3	64.7
	τH1O2CO1	0.0	−0.5	−1.7
(T3)	C–N	1.579	1.676	1.598
	C–O1	1.523	1.603	1.749
	C=O2	1.253	1.229	1.217
	H1–O1	1.251	1.176	1.269
	H1–N	1.317	1.220	1.220
	∠NCO1	85.2	82.0	82.2
	∠NCO2	114.9	118.2	117.4
	∠H1NC	80.3	73.6	80.0
	∠H1O1C	84.7	77.8	72.9
	τH1O1CN	0.6	0.8	4.1
(INT)	C–N	1.474	1.482	1.428
	C–O1	1.397	1.426	1.418
	C–O2	1.405	1.434	1.421
	∠NCO1	110.6	111.7	112.2
	∠NCO2	109.1	108.2	105.3
	∠H1O1CN	32.8	44.1	30.7
	∠H2NCO1	−95.6	−88.3	−124.6
	∠H2NCO2	24.3	33.7	−4.7
	τH3O2CO1	−61.2	−51.2	−35.1

[a] (T1), (T2), (T3), and (INT) are transition states 1, 2, 3, and intermediate, respectively. See Figures 1 and 2 for the structures. [b] Bond length (X–Y or X=Y) in Å; bond angle (∠XYZ) and dihedral angle (τWXYZ) in degrees, where W, X, Y, and Z refer to atoms as in Figures 1 and 2.

place through a stable or metastable intermediate (INT). The first step, reactant to intermediate, represents C–N bond formation through a nucleophilic attack of the nitrogen on a carbon atom and simultaneous hydrogen transfer from ammonia to a carbonyl oxygen atom. In the second step, intermediate to product, a water molecule is released by C–O and O–H bond cleavages.

In the second case, the reaction is concerted: both C–N bond formation and release of water by N–H and C–O bond cleavages take place simultaneously. In contrast to the first mechanism, in which a hydrogen atom is transferred to carbonyl oxygen from the ammonia, the concerted mechanism involves transfer of hydrogen to the hydroxyl oxygen.

Methods and Results

To characterize these two reaction mechanisms, the following approach was taken. First, a two-dimensional potential energy surface was calculated using MNDO. Two degrees of freedom were chosen as independent variables, and the remaining degrees of freedom for each independent variable were optimized. The results were used to help identify a probable reaction pathway and also to locate possible transition states and intermediates on the energy surface. Analytical gradient methods were then used to more rigorously explore the energy surface, where all degrees of freedom were used for geometry optimization. Both MNDO and ab initio methods using STO-3G and 3-21G basis sets (convergence of root mean square of gradients is 0.0003 hartree/bohr or radian) were used to locate the minima, corresponding to reactant, intermediate, and product, and saddle points, corresponding to transition states. All transition states were identified by finding one negative eigenvalue of the analytic force constant matrix.

Table II. Net Positive Charge on Incoming (NH_3) and Leaving (H_2O) Molecules at Transition States

state	molecule	charge[a] MNDO	STO-3G	3-21G
(T1)	(NH_3)	0.28	0.21	0.25
(T2)	(H_2O)	0.20	0.14	0.02
(T3)	(NH_3)	0.23	0.21	0.27
	(H_2O)	0.18	0.17	0.09

[a] Unit of charge = $+e$.

Table III. Effect of Correlation on the Relative Energies[a]

basis set	(T1)	(T2)	(T3)	(INT)	(R)
3-21G (MP2-HF)	−2.6	−11.3	−13.0	10.3	2.7
6-31G (MP2-HF)	−5.5	−11.2	−14.9	7.9	2.1
6-31G* (MP2-HF)	−15.1	−12.4	−21.8	−1.0	−0.7
6-31G** (MP2-HF)	−14.4	−11.7	−21.2	−1.0	−0.1
6-31G** (MP3-HF)	−12.9	−6.0	−15.2	−4.1	0.4
6-31G** (MP4-HF)	−11.7	−8.4	−16.3	−1.3	0.3

[a] The differences between perturbative and HF energies (in kcal/mol) are given. All the energies are relative to the energy of reactant, except that the energies of (T2) are relative to those of (INT). The energies of the product relative to those of the reactant are given in the last column. All the geometries were obtained with HF/3-21G.

Table IV. Effects of Basis Set Size and Polarization on Relative Energies[a]

basis set	(T1)	(T2)	(T3)	(INT)
HF/6-31G–HF/3-21G	8.7	2.7	10.0	2.2
HF/6-31G*–HF/6-31G	7.9	5.9	12.7	9.5
HF/6-31G**–HF/6-31G	6.3	4.4	11.2	8.1

[a] The differences in HF energies (in kcal/mol) with different basis sets are given. See also footnote *a* in Table III for the definition of the relative energies. All the geometries were obtained at HF/3-21G.

The optimized geometries found by both methods for the transition states and intermediate are given in Table I. The net positive charges of incoming NH_3 and leaving H_2O molecules at the transition states are given in Table II.

The STO-3G and 3-21G optimized geometries were then used for single-point energy calculations with more extensive basis sets and including correlation effects. Specifically 6-31G, 6-31G* (6-31G + d-type polarization functions on heavy atoms), and 6-31G** (6-31G* + p-type polarization functions on hydrogen atoms) basis sets were used for single-point calculation with 3-21G optimized geometries, and 3-21G and 6-31G basis sets with STO-3G optimized geometries.

The effects of valence electron correlation were incorporated at the levels of second (MP2), third (MP3), and fourth (MP4) order Møller–Plesset perturbation theory using an expansion developed by Pople and colleagues, with the 6-31G** basis set and 3-21G optimized geometries. MP4 was treated in the space of single, double, and quadruple substitutions, i.e., MP4 (SDQ), relative to a closed-shell HF wave function, and no account was taken of triple substitution. With all the smaller basis sets used here, MP2 calculations were also carried out in order to see the direction of the correlation effects on the relative stabilities among the reaction species. These results and the effects of basis set size and polarization are summarized in Tables III and IV, respectively. While no comparison of results from Møller–Plesset approximation and configuration interaction calculations was made in this study, such comparison exists in the literature for a number of different types of reactions. For example, comparative studies of results from Møller–Plesset perturbation and configuration interaction with single and double substituents were made for dissociation,[10]

Table V. Ab Initio Calculations on Relative Energies[a]

method[b]	(T1) $\Delta U_1^{\ddagger}$ ($\Delta G_1^{\ddagger}$)	(T2) $\Delta U_2^{\ddagger}$ ($\Delta G_2^{\ddagger}$)	(INT) ΔU_i (ΔG_i)	(T3) $\Delta U_3^{\ddagger}$ ($\Delta G_3^{\ddagger}$)	(R) ΔU_r (ΔG_r)
HF/STO-3G//A	50.7 (61.8)	78.1 (75.2)	−25.6 (−12.5)	57.8 (68.4)	9.8 (9.4)
MP2/STO-3G//A	53.5 (64.6)	56.9 (54.0)	−1.5 (11.6)	44.7 (55.3)	13.2 (12.8)
HF/3-21G//B	38.3 (49.4)	43.1 (40.2)	−5.7 (7.4)	42.0 (52.6)	1.0 (0.6)
MP2/3-21G//B	35.7 (46.8)	31.8 (28.9)	4.6 (17.7)	29.9 (40.5)	3.7 (3.3)
HF/6-31G//B	47.0 (58.1)	45.8 (42.9)	−3.5 (9.6)	52.0 (62.6)	−6.0 (−6.4)
MP2/6-31G//B	41.5 (52.6)	34.6 (31.7)	4.4 (17.5)	37.1 (47.7)	−3.9 (−4.3)
HF/6-31G*//B	54.9 (66.0)	51.7 (48.8)	6.0 (19.1)	64.7 (75.3)	1.8 (1.4)
MP2/6-31G*//B	39.8 (50.9)	39.3 (36.4)	5.0 (18.1)	42.9 (53.5)	1.1 (0.7)
HF/6-31G**//B	53.3 (64.4)	50.2 (47.3)	4.6 (17.7)	63.2 (73.8)	0.1 (−0.3)
MP2/6-31G**//B	38.9 (50.0)	38.5 (35.6)	3.6 (16.7)	42.0 (52.6)	0.0 (−0.4)
MP3/6-31G**//B	40.4 (51.5)	44.2 (41.3)	0.5 (13.6)	48.0 (58.6)	−0.3 (−0.7)
MP4/6-31G**//B	41.6 (52.7)	41.8 (38.9)	3.3 (16.4)	46.9 (57.5)	0.4 (0.0)
HF/3-21G//A	40.7 (51.8)	44.4 (41.5)	−3.7 (9.4)	43.2 (54.4)	5.4 (5.0)
HF/6-31G//A	42.2 (53.3)	47.8 (44.9)	−0.6 (12.5)	54.6 (65.2)	−1.2 (−1.6)
method	$T\Delta S_1^{\ddagger}$	$T\Delta S_2^{\ddagger}$	$T\Delta S_i$	$T\Delta S_3^{\ddagger}$	$T\Delta S_r$
HF/STO-3G//A	−11.6	−1.0	−10.6	−12.0	0.1
HF/3-21G//B	−11.5	−0.6	−10.7	−11.4	0.0
method	$\Delta V_1^{\ddagger}$	$\Delta V_2^{\ddagger}$	ΔV_i	$\Delta V_3^{\ddagger}$	ΔV_r
HF/STO-3G//A	−0.4	−3.3	2.9	0.2	−1.0
HF/3-21G//B	−0.4	−3.5	2.4	−0.8	−0.4

[a] All relative energies, ΔU, ΔG, $T\Delta S$, ΔV are in kcal/mol. G (free energy), S (entropy), and V (sum of the translational, rotational, and vibrational enthalpies) are calculated at 298 K and 1 atm. ΔU is the Hartree–Fock (HF) or perturbative (MP) energy. All the energies are relative to the energy of reactant, except that the energies at (T2) are relative to those at (INT). The energies of the product relative to those of the reactant are given in the last column. Note that $\Delta G = \Delta U - T\Delta S + \Delta V$. [b] The methods and basis sets used for geometry optimization and single-point energy calculation are given at the right and left sides of //, respectively, where A = HF/STO-3G and B = 3-21G. The fourth-order Møller–Plesset calculation (MP4) includes all single, double, and quadruple substitutions, i.e., MP4 (SDQ).

isomerization,[11] and rearrangement[12] reactions. In each case, an excellent agreement was obtained not only for energy of reaction but also for energy of activation.

MNDO, STO-3G, and 3-21G optimized geometries were used as the basis for calculating translational (tr), rotational (rot) and vibrational (vib) contributions to the relative enthalpies and entropies. The formulas for these entities are derived from the molecular partition function.[13]

The relative free energy at temperature T is given by the following equations

$$\Delta G(T) = \Delta U + \Delta H_{tr}(T) + \Delta H_{rot}(T) + \Delta H_{vib}(T) - T\Delta S(T)$$

$$\Delta S(T) = \Delta S_{tr}(T) + \Delta S_{rot}(T) + \Delta S_{vib}(T)$$

where ΔU in the ab initio calculation is the Hartree–Fock or perturbative potential energy difference and in the MNDO calculation is $\Delta H_f°$, both exclusive of the vibrational zero-point energy which is included in $\Delta H_{vib}(T)$. Relative free energies, entropies, and thermal energies calculated with ab initio and MNDO methods (at 298.15 K and 1 atm) are summarized in Tables V and VI, respectively.

Discussion

Geometries. For both the stepwise and concerted mechanisms of amide bond formation, the first transition state involves simultaneous nucleophilic attack of the amine nitrogen on the carbonyl carbon (i.e., partial C–N bond formation) and partial transfer of an amine hydrogen atom to the carboxylic acid oxygen atom (i.e., partial O–H bond formation). No transition state involving only nucleophilic attack of the amine nitrogen on the carbonyl carbon was found.

Table VI. MNDO Calculations of Relative Energies[a]

	(T1)	(T2)	(INT)	(T3)	(R)
ΔH	61.2	82.5	−7.8	77.7	−2.3
$T\Delta S$	−11.8	−1.1	−10.4	−12.0	0.1
ΔV	−0.2	−3.8	2.8	−0.6	−0.8
ΔG	72.8	79.8	5.4	89.1	−3.0

[a] All relative energies (see footnote *a* in Table III for definition) are in kcal/mol calculated at 298 K and 1 atm. No thermal energy (ΔV) corrections are made for ΔH.

In the stepwise mechanism of amide bond formation, both MNDO and ab initio methods yielded two transition states, (T1) and (T2), with planar, four-membered rings and an sp^2 planar hybridization around the carbon atom but fairly distorted toward a tetrahedral configuration.

The overall (T1) structure is quite similar in all MNDO, STO-3G, and 3-21G optimized geometries. In this transition state, the partially formed H–O bond was found to be significantly longer than the N–H bond to be broken in all three optimized geometries. Thus, all methods used indicate that this transition state more closely resembles the reactant than the intermediate formed, which is consistent with the Hammond postulate in the sense that the intermediate was found to have lower internal energy than the reactant at these levels of calculations. One significant difference between methods is in the partially formed C–N bond. From the difference in C–N bond length between (T1) and the intermediate calculated by each method, i.e., 0.111 (MNDO), 0.274 (STO-3G), and 0.178 (3-21G) Å, the STO-3G transition state is seen to be furthest from the intermediate. It is interesting to note that the amount of electron transfer from ammonia to formic acid is quite similar in the three (T1) structures, i.e., 0.28 (MNDO), 0.21 (STO-3G), and 0.25 (3-21G) electrons.

For the second transition state (T2), a fairly large difference is observed in the timing of the departure of the water molecule among the three optimized geometries, being most complete in the 3-21G calculation. In the MNDO and STO-3G structures, the C–O2 bond breaking has progressed less, and H1–O1 bond

(10) Pople, J. A.; Seeger, R.; Krishnan, R. *Int. J. Quantum Chem. Symp.* **1977**, *11*, 149.
(11) (a) Frisch, M. J.; Krishnan, R.; Pople, J. A. *J. Phys. Chem.* **1981**, *85*, 1467. (b) Harding, L. B.; Schlegel, H. B.; Krishnan, R.; Pople, J. A. *J. Phys. Chem.* **1980**, 84, 3394. (c) Goddard, J. D.; Yamaguchi, Y.; Schaefer, H. F. *J. Chem. Phys.* **1981**, *75*, 3459.
(12) (a) Krishnan, R.; Frisch, M. J.; Pople, J. A. *Chem. Phys. Lett.* **1981**, *79*, 408. (b) Dyksta, C. E.; Schaefer, H. F. *J. Am. Chem. Soc.* **1978**, *100*, 1378.
(13) Hertzberg, G. "Molecular Spectra and Molecular Structure: II. Infrared and Raman Spectra of Polyatomic Molecules"; Van Nostrand Co.: Toronto, 1968; Chapter 5.

cleavage and H1–O2 bond formation progressed more than in the 3-21G case. This difference in timing is also indicated in the extent of net positive charge remaining on the leaving water molecule, i.e., 0.20 (MNDO), 0.14 (STO-3G), and 0.02 (3-21G).

For the intermediate, all three optimized geometries give a regular sp^3 tetrahedral configuration around the carbon atom and a nearly eclipsed conformation between the NH_2 group and the C–O bond. The overall agreement in the structural parameters between the MNDO and STO-3G optimized geometries is fairly good. The 3-21G optimized geometry has somewhat larger differences from the other two geometries mainly in the C–N bond length and dihedral angles around the C–N and C–O bonds.

The transition state (T3) calculated by both the MNDO and ab initio methods for the concerted mechanism also has a planar four-membered ring and a distorted tetrahedral configuration around the carbonyl carbon atom. Again, both MNDO and STO-3G optimized geometries of the transition state (T3) show that C–O1 bond cleavage has progressed less than in the 3-21G case, which is also indicated in the net positive charge on the leaving water molecule, i.e., 0.18 (MNDO), 0.17 (STo-3G), and 0.09 (3-21G). The amounts of electron transfer from ammonia to formic acid are also comparable to those found in the transition state (T1). As is expected, all three transition states are much more polar than the intermediate state. The calculated dipole moments, using the 6-31G** basis set, with 3-21G optimized geometries are 4.00, 3.57, 3.98, and 0.87 D for the transition states (T1), (T2), (T3), and the intermediate, respectively.

Energetics. Throughout the following discussions all energy comparisons refer to free energies, unless otherwise noted. All the energies given in Tables III–VI are relative to the energy of the reactant, except that the energies at (T2) are relative to those of the (INT). Table V summarizes the Hartree–Fock (HF) and perturbative energies (ΔU) and free energy (ΔG) calculated for all the stationary points of both reaction pathways at all levels of calculation. For ΔG values listed in Table V calculated by the ab initio method, entropies and thermal energies calculated with 3-21G basis set were used. As shown in Table V, these values are almost the same as those calculated with the STO-3G basis set. Experimental values of $\Delta G_r = -0.3$ and $T\Delta S_r = -0.4$ kcal/mol were calculated from the experimental heats of formation and entropies of the reactant and product molecules in the gas phase.[14] These results are in very good agreement with the results of our highest level calculations, i.e., $\Delta G_r = 0.0$ (MP4/6-31G**) and $T\Delta S_r = 0.0$ kcal/mol.

In Table III, the effect of correlation on the stationary point energies is given as the difference between the perturbative and Hartree–Fock energies at various basis sets. For calculations which include polarization, significantly large correlation effects are observed which tend to lower the relative energies for all three transition states (T1), (T2), and (T3), while only small effects are seen for stable reaction species.

Despite the close structural similarity between the transition states (T1) and (T3), the larger correlation effect observed with (T3) is understandable considering the total number of bonds cleaved and formed, i.e., three for (T1) and four for (T3). On the other hand, the larger effect of correlation on the transition state (T1) compared to (T2) can be attributable to the larger structural changes in the transformation of the reactant to (T1) than in the transformation of the intermediate to (T2).

It is interesting to note that even for the 3-21G and 6-31G basis sets, the directions of correlation effects on the activation energies are the same as those observed for larger basis sets, though the correlation energy for (T1) is fairly underestimated compared with those for (T2) and (T3) with the smaller basis sets.

In comparing the 6-31G* and 6-31G** basis sets, it is seen that correlation energies at the MP2 level differ slightly (a maximum of 0.7 kcal/mol), but the differences in the correlation energies between the transition states remain the same for both of these basis sets. A comparison of MP2 and MP4 treatments of correlation energies calculated with 6-31G** basis set shows that the Møller–Plesset expansion terminated at second-order results in an overestimation of the correlation energies by 3–5 kcal/mol for the transition states.

Table IV summarizes the effects of the basis set size and polarization on the stationary point energies. Contrary to correlation effects, which lower the activation energy at every level, increasing basis set size from 3-21G to 6-31G, and addition of d polarization functions to the 6-31G basis set, increases the relative energies for both the transition states and the intermediate. However, a decrease in activation energies, though only slight (1.5 kcal/mol), is obtained by the addition of p polarization functions to the H atoms in the 6-31G* basis set. This decrease is most likely due to the increased stabilization of multiple bonds formed by the H1 atoms in the four-membered ring transition states.

For all transition states, correlation and polarization effects are in opposite directions, but both affect each transition state in the same order (T3) > (T1) > (T2). Thus by cancellation, the net effect on these activation energies is very similar, i.e., −5.1, −4.0, and −5.4 kcal/mol for (T3), (T2) and (T1), respectively. In consequence of the opposite effects of correlation and polarization, HF/6-31G results for the transition states are very similar to the highest level MP4/6-31G** calculations we have performed, as shown in Table V.

The higher level of calculations performed (e.g., HF/6-31G, MP2/6-31G*, MP2/6-31G**, MP3/6-31G**, MP4/6-31G**) predicts an intermediate less stable than the reactant (i.e., $\Delta G_i > 0$) and the order of activation energies $\Delta G_2^{\ddagger} < \Delta G_1^{\ddagger} < \Delta G_3^{\ddagger}$. All of these results are qualitatively reversed in the HF/STO-3G results (see row 1 in Table V). However, the single point energy calculation at the 3-21G or 6-31G level, using the optimized geometry obtained with an STO-3G basis set, i.e., HF/3-21G//HF/STO-3G or HF/6-31G//HF/STO-31G, makes them consistent with the results obtained from higher level calculations. Thus, for a larger system such as peptide bond formation between two glycine molecules, a reasonable level of calculations would be HF/3-21G//HF/STO-3G or HF/6-31G//HF/STO-31G, i.e., use of the STO-3G basis set to obtain stationary points and single point energy calculations of these species using the 3-21G or 6-31G basis set.

A comparison of the free energies of activation, $\Delta G_1^{\ddagger}$ and $\Delta G_2^{\ddagger}$, for the stepwise reaction mechanism clearly shows that the first step (i.e., nucleophilic attack by nitrogen atom on the carbonyl carbon atom) is slower than the second step. Further, since the potential energies $\Delta U_1^{\ddagger}$ and $\Delta U_2^{\ddagger}$ are nearly equal, the entropy contribution to the free energy (i.e., $T\Delta S$ of −11.5 kcal/mol to $\Delta G_1^{\ddagger}$ and −0.6 kcal/mol to $\Delta G_2^{\ddagger}$) is the most critical factor in determining which step has the larger activation energy in this mechanism. The overall rate of the reaction is determined by the free energy difference between the reactant and the highest point of the energy surface. Relative to the reactant, the highest point of the energy surface is the energy of the second transition state ($\Delta G_2^{\ddagger} + \Delta G_i^{\ddagger}$) which is greater than $\Delta G_1^{\ddagger}$ at the four highest levels of calculation. However, the small difference between these two quantities, i.e., 55.3 vs. 52.7 kcal/mol at the MP4/6-31G** level, implies that both steps nearly equally affect the overall rate of the reaction.

Comparing the two possible mechanisms of amide bond formation, the free energies of activation of both steps in the stepwise mechanism ($\Delta G_1^{\ddagger}$ and $\Delta G_2^{\ddagger} + \Delta G_i^{\ddagger}$) are calculated to be slightly lower than that for the concerted one ($\Delta G_3^{\ddagger}$) at the 6-31G** level. However, the calculated difference is too small (i.e., $\Delta G_3^{\ddagger} = 57.5$; $\Delta G_2^{\ddagger} + \Delta G_i^{\ddagger} = 55.3$ kcal/mol) to allow a definitive decision about which is the most favorable mechanism even at the highest level of theory used here, MP4/6-31G**. Because of the countereffects of polarization and correlation, and of the similar nature of the transition states (T1), (T2), and (T3), even a more sophisticated calculation with much larger basis set and full configuration interaction (CI) treatment, for example, is not likely to change our results. Thus, for amide bond formation we predict that in

(14) (a) Cox, J. D.; Pilcher, G. "Thermochemistry of Organic and Organometallic Compounds"; Academic Press: New York, 1970. (b) Stull, D. R.; Prophet, H. *Natl. Stand. Ref. Data Ser.* **1971**, *No. 37*. (c) Wagman, D. D.; Evans, W. H.; Parker, V. B.; Halow, I.; Baily, S. M.; Schumm, R. H. *Natl. Bur. Stand. Tech. Note* **1968**, *No. 270–3*.

a gas phase, or in a hydrophobic environment, the two reaction mechanisms would be equally possible and that in the stepwise reaction, although the first step would be slower, both steps affect the overall rate.

The results of the parallel MNDO calculations given in Table VI show that excellent agreement in both ΔS and thermal energies with those calculated by the ab initio method. These results also favor a stepwise reaction, with the second step rate determining. However, all the activation energies calculated with MNDO are much higher than with the ab initio method. Overestimation of the activation energy by MNDO is due mainly to the lack of direct incorporation of correlation effects. The consequence of this lack is reflected in the fact that the relative enthalpy of the intermediate suggests that it is more stable than the reactant, a result also obtained from the Hartree–Fock calculations with a small basis set.

Conclusions

Several conclusions can be drawn from this study.

(1) Stepwise and concerted reaction mechanisms of amide bond formation have been characterized which involve simultaneous nucleophilic attack of the amine on the carboxyl carbon atom and transfer of a hydrogen atom to an oxygen atom. In both the gas phase and hydrophobic environments, both the stepwise and concerted reaction mechanisms for amide bond formation would be equally competitive, with the former predicted to be slightly favored by both MNDO and a higher level of ab initio calculations. For the stepwise mechanism the first step, reactant to intermediate, is slower than the second step, intermediate to product, due mainly to the entropy contribution to the free energy of activation. However, the activation energy of the second step relative to the reactant is predicted to be slightly higher than that of the first step by both MNDO and a higher level of ab initio calculations, indicating that the overall rate-determining step for this mechanism is affected by both steps. The intermediate is found to be less stable than the reactant.

(2) Entropy contributions to free energy are much greater than thermal energy contributions. MNDO and ab initio calculations of entropy and of thermal energy are in excellent agreement with each other, but MNDO yields much higher activation energies. Neglect of correlation effect in MNDO seems to be primarily responsible for the calculated high activation energies.

(3) Correlation effects and p polarization functions lower the activation energies which are raised by d polarization functions. The total effect of correlation and polarization is to lower the activation energies by 4.0–5.4 kcal/mol; nearly equal values are calculated for each of the three transition states of interest. Therefore, the relative order of free energies of activation predicted at the highest level of theory used here is the same as that predicted by the HF/3-21G or HF/6-31G level of calculations, i.e., $\Delta G_2^{\ddagger} < \Delta G_1^{\ddagger} < \Delta G_3^{\ddagger}$.

(4) STO-3G optimized structures used for single-point calculations of activation energies at higher levels of theory yield results qualitatively identical with those from the four highest level calculations.

In subsequent studies we plan to further characterize peptide bond formation between amino acids and to investigate the role of acid–base catalysis and divalent metal ions in this process, using STO-3G optimized structures and single-point energy calculations at higher levels of theory.

Acknowledgment. Support from NASA Consortium Agreement NCA2-OR630-001 with The Rockefeller University is acknowledged. We are indebted to Dr. D. Spangler for helpful and stimulating discussions. We also thank Dr. D. DeFrees for computational help on various aspects of this work.

Registry No. Ammonia, 7664-41-7; formic acid, 64-18-6; formamide, 75-12-7.

Structural Effects on Twisted Olefin Triplet Lifetimes. Styrene Derivatives

R. A. Caldwell* and C. V. Cao

Contribution from The University of Texas at Dallas, Richardson, Texas 75080.
Received March 2, 1982

Abstract: The triplet lifetimes in methanol of a series of anisylalkenes and anisylcycloalkenes, including several phenyl analogues, have been determined by nanosecond flash kinetic absorption spectrophotometry with nitrogen laser excitation. Electron-transfer scavenging by paraquat dication, PQ^{2+}, (methyl viologen) afforded the readily detectable reduced species $PQ^{+\cdot}$. Both triplet lifetimes and rate constants for electron transfer from triplet to PQ^{2+} were determined. The results indicate that acyclic styrene triplets prefer the twisted, "1,2-biradical" structure. Lifetimes are increased by vinyl deuteration, by increasing alkylation, and by constraint within a small ring; in the absence of geometric constraints, the dominant influence on the triplet lifetimes is the extent of substitution at the double bond. Mechanisms for intersystem crossing are discussed, and the tentative conclusion is reached that nuclear motions are important.

Despite their central importance in a variety of photochemical reactions and their interest in both experimental and theoretical photophysical studies,[1] olefin triplets in fluid solution have until the relatively recent advent of nanosecond laser flash photolysis techniques been difficult to detect. Interception of stilbene triplets by azulene,[2] di-*tert*-butyl nitroxide,[3] and oxygen[4] in steady-state experiments was reported some years ago, but determination of lifetimes from such studies was subject to assumption of the relevant rate constant in each case. These studies were further complicated by the planar-twisted ($^3t \rightleftarrows {}^3p$) equilibrium for

(1) See Saltiel, J.; Charlton, J. L. In "Rearrangements in Ground and Excited States"; de Mayo, P., Ed.; Academic Press: New York, 1980, Vol. III, p 25ff.

(2) Hammond, G. S.; Saltiel, J.; Lamola, A. A.; Turro, N. J.; Bradshaw, J. S.; Cowan, D. O.; Counsell, R. C.; Vogt, V.; Dalton, C. *J. Am. Chem. Soc.* **1964**, *86*, 3197.

(3) Caldwell, R. A.; Schwezel, R. E. *J. Am. Chem. Soc.* **1973**, *95*, 1382.

(4) Saltiel, J.; Thomas, B. *J. Am. Chem. Soc.* **1974**, *96*, 5660.

0002-7863/82/1504-6174$01.25/0